Angewandte Chemie
International Edition

Conformation Analysis

International Edition: DOI: 10.1002/anie.201506898
German Edition: DOI: 10.1002/ange.201506898

Magnetic Control of Macromolecular Conformations in Supramolecular Anionic Polysaccharide–Iron Complexes

*Larissa Schefer, Ariane Bulant, Christophe Zeder, Abhijit Saha, and Raffaele Mezzenga**

Abstract: *The anionic iota carrageenan polysaccharide is enriched with* Fe^{II} *and* Fe^{III} *by ion exchange against* $FeSO_4$ *and* $FeCl_3$*. With divalent iron, portions of polymer chains undergo a secondary structure transition from random coils to single helices. The single-chain macromolecular conformations can be manipulated by an external magnetic field: upon exposure to 1.1 T, the helical portions exhibit 1.5-fold stiffening and 1.1-fold stretching, whereas the coil conformations respond much less as a result of lower contents of condensed iron ions. Along with the coil–helix transition, the trivalent iron triggers the formation of superstructures. The applicability of iron-enriched iota carrageenan as functional ingredient for food fortification is tested by free* Fe^{2+} *and* Fe^{3+} *contents, respectively, with the most promising iota-*Fe^{III} *yielding 53% of bound iron, which is due to the superstructures, where the ferric ions are chelated by the supramolecularly self-assembled polymer host.*

Carrageenans are naturally occurring sulfated linear galactan polysaccharides, which constitute the cell walls of red seaweeds.[1] The three major types—kappa, iota, and lambda—find application in food, cosmetic, and pharmaceutical product formulations, where they serve as gelling agents, thickeners, and excipients.[1] Polyelectrolytes, such as the anionic carrageenans, change their molecular conformation depending on chemical traits of the polymer as well as properties of their ionic environments.[2] Various studies of carrageenans in varying ionic conditions and temperature, revealed order–disorder conformational transitions,[3] and self-association[4] leading to gelation.[5] Alkali and alkaline earth metal cations such as Li^+,[3c,4a,5a] Na^+,[3a–c,e,f,4,5a,b,e] K^+,[3a,b,d,4c,5a–e] Cs^+,[4b,5a,c] Rb^+,[3b,5a] and Ca^{2+}[4c,5b–e] were studied intensively, whereas the effects of transition metals such as iron[6] have remained largely unexplored.

Iron compounds are ubiquitous in industrial applications, have vital functions in biological processes, and are essential in the human diet.[7] If the human body lacks sufficient amounts, iron deficiency and anemia develop, which are prevailing global health issues.[8a] To overcome this problem, iron supplementation and food fortification strategies are being actively pursued.[8] The application of carrageenan as food-grade functional polymer hosts for complexation of iron ions into supramolecular structures could be an alternative strategy of immediate practical significance.

Herein, we have developed a method to transform commercial iota carrageenan into the iron form by ion exchange against $FeSO_4$ and $FeCl_3$. Flame atomic absorption spectrophotometry (AAS) confirms the transformation to the iron form, whereas all other ionic species remain at very low concentrations (Supporting Information, Table S1). Using this procedure, iron contents of 101 and 119 mg g^{-1} with respect to dry weight of purified iota-Fe^{II} and iota-Fe^{III}, respectively, are obtained. The molecular conformations of the purified iota carrageenans are visualized by atomic force microscopy (AFM; Figure 1), in direct analogy with our earlier work on the secondary structure formation of carrageenans exposed to NaCl, KCl, and $CaCl_2$.[3e,f,4c] AFM imaging of iota-Fe^{II} reveals a coexistence of two distinct polymer

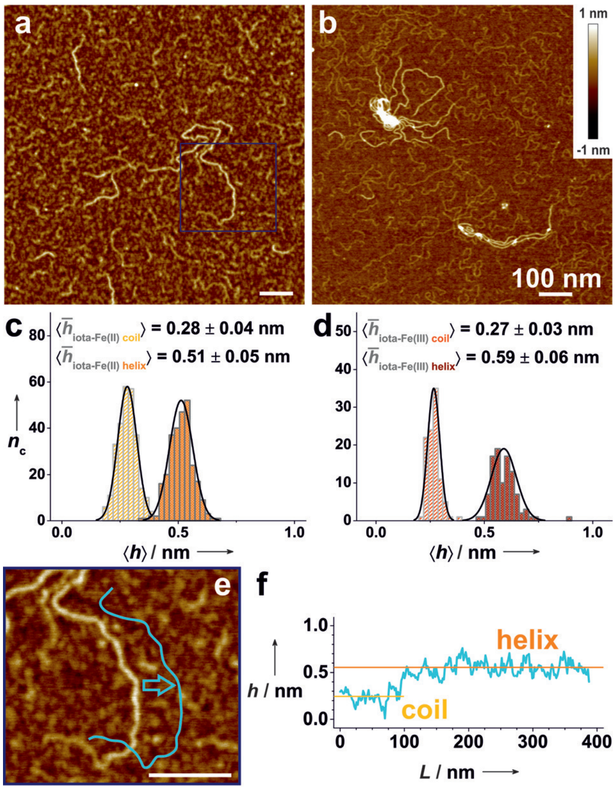

Figure 1. AFM height images of a) iota-Fe^{II} and b) iota-Fe^{III} as obtained after ion exchange with $FeSO_4$ and $FeCl_3$, respectively, with c,d) corresponding height histograms of averaged heights $\langle h \rangle$ of number of chains n_c in random coil and helical conformation. e) Magnification of the blue rectangle in (a) and f) height profile of the polymer indicated in (e). Scale bar of 100 nm and color bar correspond to all AFM images.

---

[*] L. Schefer, A. Bulant, C. Zeder, Dr. A. Saha, Prof. Dr. R. Mezzenga
Department of Health Sciences & Technology, ETH Zürich
Schmelzbergstrasse 9, LFO E23, 8092 Zürich (Switzerland)
E-mail: raffaele.mezzenga@hest.ethz.ch

Supporting information for this article is available on the WWW under http://dx.doi.org/10.1002/anie.201506898.

populations (Figure 1 a). Mean average chain heights of 0.28 ± 0.04 and 0.51 ± 0.05 nm, corresponding to random coils and single helices, respectively,[3e,f] are estimated by statistical analysis on over 100 polymer traces for each conformational state (Figure 1 c). The appearance of partial helical conformations after the purification we observed as well[4c] by ion exchange against $CaCl_2$ and is a result of the enhanced screening of divalent counterions, which enable the conformational transition at room temperature already upon ion exchange.

The AFM surface topographies of iota-Fe^{III} also reveal coexisting random coils and single helices with mean average chain heights of 0.27 ± 0.03 and 0.59 ± 0.06 nm, respectively (Figure 1 b,d). Moreover, the single helices self-associate in supramolecular clusters of a rich polymorphism (Figure 2; Supporting Information, Figure S1), with superstructures consisting of an amorphous dense core (Supporting Information, Figure S2) and a brush region of single helices. The morphologies resemble packing of DNA in presence of condensing agents of predominantly higher valence.[9] The trivalent iron therefore enables supramolecular cluster formation, which is potentially due to multiple interaction sites of counterions with multiple carrageenan chains.

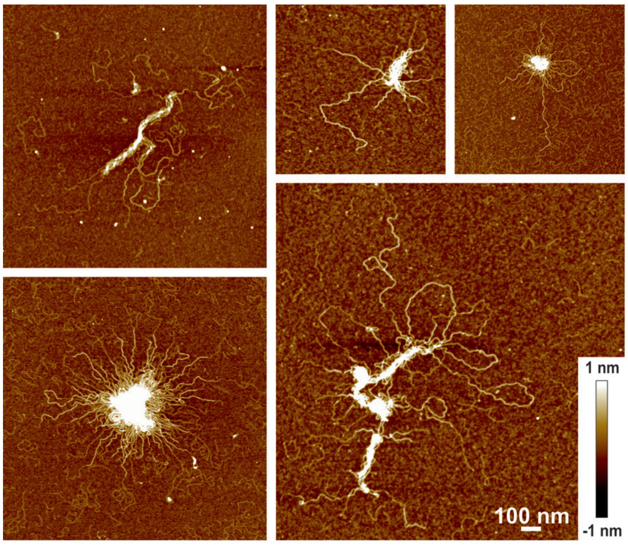

Figure 2. AFM height images of iota-Fe^{III} superstructures as obtained after ion exchange with $FeCl_3$. Scale and color bars correspond to all images.

The successful implementation of iron-enriched carrageenans for food fortification requires the assessment of the free iron content, that is, the quantity of iron that is not bound tightly and therefore might be released into the food matrix where undesirable color changes and off-flavors can result.[8a] As test reagents, ferrozine[10] and ammonium thiocyanate[11] were used, which form intensely colored complexes with Fe^{2+} and Fe^{3+}, respectively. Iota-Fe^{II} exhibits an intense change in color in presence of ferrozine, signifying a high quantity of free iron. Iota-Fe^{III}, on the other hand, yields only a slight color change in presence of ammonium thiocyanate, suggesting a rather high fraction of bound iron (Supporting Information, Figure S3), in agreement with the previously reported[12] chelation of Fe^{3+} in acidic conditions. Spectrophotometric determination (Supporting Information, Figure S4) quantifies a total of 53 % bound iron in iota-Fe^{III} (Supporting Information, Table S2), suggesting a good binding which may be suitable for food fortification. Instead, iota-Fe^{II} with only 6 % bound iron (Supporting Information, Table S2), does not compete with its trivalent counterpart. The divergent performance of iota-Fe^{II} and iota-Fe^{III}, respectively, may result from the capability of the latter to induce self-association into condensed superstructures which efficiently chelate trivalent iron ions with the higher charge-to-radius ratio, thus the higher affinity to complex with hard oxygen ligands such as sulfates[13] (Figure 2; Supporting Information, Figure S1).

The presence of iron condensed on carrageenans opens the way for unprecedented functionalities well beyond food fortification. For example, iron nanoparticle–carrageenan nanohybrids were reported to feature catalytic activity.[14] The magnetic susceptibility of iron furthermore allows the noninvasive manipulation of soft matter by using magnetic fields.[15] Previous strategies have focused on in situ synthesis[14b,16] or incorporation[14a,17] of inorganic magnetic nanoparticles to address the low magnetic susceptibility of organic matter; thereby, carrageenan gels with magnetically tunable elasticity[17a] and superparamagnetic property[16] were achieved. Magnetic manipulation of single polymer chains doped with iron ions, has, however, not yet been reported to the best of our knowledge, which motivated the investigation of the magnetic susceptibility of Fe^{II}-enriched iota carrageenan and their response to magnetic fields. This is assessed by depositing iota-Fe^{II} supramolecular complexes onto a (3-aminopropyl)triethoxysilane (APTES)-modified mica substrate while applying a moderate external magnetic field of 1.1 T oriented parallel to the substrate plane using a Halbach magnet (Figure 3 a). AFM imaging of the sample deposited in presence (magnet) and absence (control) of the magnetic field displays homogeneously distributed polymers with coexisting random coil and helical conformations (Figure 3 b; see the Supporting Information, Figure S5 for full images). The single helices appear less flexible and more stretched and

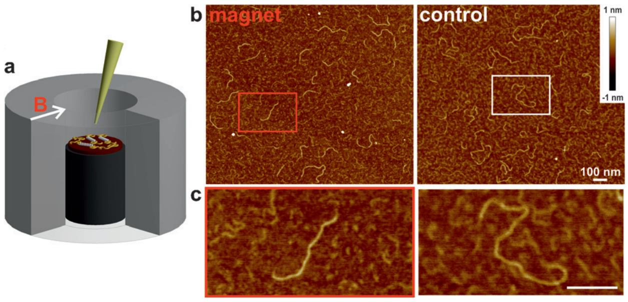

Figure 3. a) Setup of the magnetic susceptibility experiment with a magnetic field of 1.1 T applied in the plane of the substrate during sample preparation. b) Representative AFM height images of iota-Fe^{II} prepared in presence (magnet) and absence (control) of the magnet. c) Magnification of frames in (b) highlighting more stretched and stiffer chains due to the magnetic field. Scale bar of 100 nm and color bar correspond to all AFM images.

extended when the magnet is applied. Instead, no change is noticeable for the random coils, suggesting the preservation of the macromolecular conformation irrespective of the magnetic field. To quantify this effect, over 500 polymers in random coil and helical conformation, respectively, were traced by applying the open-source FiberApp tracking routine[18] on the AFM images. From the contours of the fibers, the persistence length L_p, reflecting the stiffness of the polymers, is calculated using the two-dimensional wormlike chain (WLC) model,[19] following $\langle R^2\rangle = 4L_p(L-2L_p(1-\exp(-L/2L_p)))$, where $\langle R^2\rangle$ is the average 2D mean square end-to-end distance and L the internal contour length between two points on the polymer for which $\langle R^2\rangle$ is calculated (Figure 4a; see the Supporting Information, Figure S6 for height and length distributions). In the presence of the magnetic field, the helical polymers, with $L_p = 37.1 \pm 0.1$ nm, are stiffer compared to 25.4 ± 0.1 nm in the control sample without the magnet, indicating a 1.5-fold stiffening of the chains. The random coils, in contrast, stiffen to a much weaker extent from 22.3 ± 0.1 to 25.1 ± 0.1 nm. Chain portions with ion-induced helical conformation therefore respond significantly to the magnetic field, whereas random coils stiffen only marginally. This is consistent with the expectation of higher ion fractions in helical chain portions, that is, high enough to induce a coil–helix transition, whereas chain portions with less condensed ions, that is, the random coils, do not possess significant magnetic susceptibility to respond to the magnetic field. Polymer stiffness was previously altered by ionic environment[3f] or solvent polarity,[20] but coupled secondary structure formation and magnetic tuning of polymer chains by condensed iron ions is reported here for the first time.

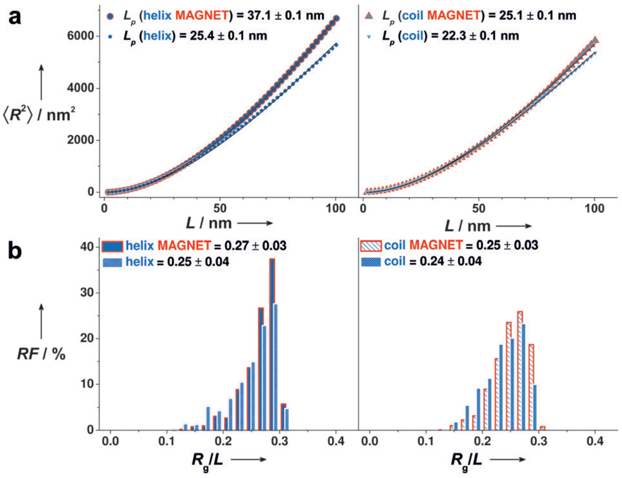

Figure 4. Statistical analysis of helical and random coil polymer traces extracted from AFM images obtained in presence and absence of a magnetic field. a) Measured mean square end-to-end distance $\langle R^2\rangle$ vs internal contour length L quantifying a stiffening of helical chains owing to the magnetic field (left), while random coils remain fairly unchanged (right). The 2D WLC fits are colored in black. b) Probability histograms with relative frequencies *RF* of radii of gyration R_g normalized by L of helical (left) and random coil (right) polymer portions indicate a stretching of the helical chains.

To quantify whether the polymer stiffening is paired by a stretching, we furthermore extracted by statistical analysis the two-dimensional radius of gyration, R_g, of the polymers. Probability histograms of R_g normalized by the polymer contour length L indicate a slight increase of the arithmetical means of the distributions for the helical conformations from 0.25 ± 0.04 to 0.27 ± 0.03 when the magnet is applied, whereas the random coils again remain essentially constant (Figure 4b; see the Supporting Information, Figure S7 for the corresponding count histograms). The iota-Fe^{II} in helical conformation therefore not only exhibit enhanced intrinsic stiffening but also global stretching that is due to the magnetic field, thereby offering new possibilities to stretch single polymer chains beyond manipulation by flow,[21a] optical tweezers,[21b] or electrophoresis.[21c] The stiffening and stretching of the chains is expected to arise from the presence of a magnetic field gradient changing from 0 to 1.1 T during the sample deposition, and/or by the inhomogeneous distribution of condensed ions along the polymer chains, as revealed by the coexistence of random coils and single helices. We anticipate that by engineering the external magnetic field, for example, by introducing strong gradients, an even more pronounced magnetic response of the helical iota-Fe^{II} chains may result.

In summary, supramolecular complexation of the anionic food polysaccharide iota carrageenan with ferrous and ferric ions was achieved by dialysis and ion exchange against $FeSO_4$ and $FeCl_3$, respectively. With the divalent counterion, parts of the polymer undergo a transition from a random coil to a single helical conformation. Besides the ion-induced coil–helix transition, the trivalent counterions furthermore trigger superstructure formation by sequestering the ferric ions more efficiently compared to the ferrous ions, which is reflected in the higher content of bound iron in the iota-Fe^{III} complex. Although further tests are needed to evaluate in vivo bioavailability and sensory changes in real food matrices,[8a] the present results indicate a potential role of carrageenan–iron complexes as functional ingredients for iron food fortification. By statistical analysis of polymer contours extracted from AFM images, we uncovered a magnetically triggered local stiffening and global stretching of the helical iota-Fe^{II} chains. The magnetic response of the ferrous ion-enriched polysaccharide is promising as the application of an external magnetic field allows a noninvasive, facile and cost-effective manipulation of biomacromolecules. This offers an alternative strategy for the magnetic manipulation of individual biopolymer chains, which does not require introducing inorganic magnetic nanoparticles.

Acknowledgements

We thank Martin Michel and Nico Galaffu (Nestlé Research Center) for stimulating discussions and technical support for free iron experiments. Beat Eberle is acknowledged for assistance in figure design. The Swiss National Science Foundation (SNSF) is acknowledged for financial support.

Keywords: atomic force microscopy · carbohydrates · coil–helix transition · conformation analysis · magnetic manipulation

How to cite: *Angew. Chem. Int. Ed.* **2015**, *54*, 13289–13292
Angew. Chem. **2015**, *127*, 13487–13490

---

[1] a) F. van de Velde, G. A. de Ruiter, *Biopolymers Online* **2005**; b) V. L. Campo, D. F. Kawano, D. B. da Silva, Jr., I. Carvalho, *Carbohydr. Polym.* **2009**, *77*, 167–180.

[2] A. V. Dobrynin, M. Rubinstein, *Prog. Polym. Sci.* **2005**, *30*, 1049–1118.

[3] a) I. T. Norton, D. M. Goodall, *J. Chem. Soc. Faraday Trans. 1* **1983**, *79*, 2475–2488; b) P. S. Belton, B. J. Goodfellow, R. H. Wilson, *Macromolecules* **1989**, *22*, 1636–1642; c) K. Bongaerts, S. Paoletti, B. Denef, K. Vanneste, F. Cuppo, H. Reynaers, *Macromolecules* **2000**, *33*, 8709–8719; d) V. Y. Grinberg, N. V. Grinberg, A. I. Usov, N. P. Shusharina, A. R. Khokhlov, K. G. de Kruif, *Biomacromolecules* **2001**, *2*, 864–873; e) L. Schefer, J. Adamcik, R. Mezzenga, *Angew. Chem. Int. Ed.* **2014**, *53*, 5376–5379; *Angew. Chem.* **2014**, *126*, 5480–5483; f) L. Schefer, I. Usov, R. Mezzenga, *Biomacromolecules* **2015**, *16*, 985–991.

[4] a) N. Mischenko, B. Denef, M. H. J. Koch, H. Reynaers, *Int. J. Biol. Macromol.* **1996**, *19*, 185–194; b) L. Piculell, J. Borgström, I. S. Chronakis, P.-O. Quist, C. Viebke, *Int. J. Biol. Macromol.* **1997**, *21*, 141–153; c) L. Schefer, J. Adamcik, M. Diener, R. Mezzenga, *Nanoscale* **2015**, DOI: 10.1039/C5NR04525H.

[5] a) E. R. Morris, D. A. Rees, G. Robinson, *J. Mol. Biol.* **1980**, *138*, 349–362; b) A.-M. Hermansson, E. Eriksson, E. Jordansson, *Carbohydr. Polym.* **1991**, *16*, 297–320; c) M. Takemasa, A. Chiba, M. Date, *Macromolecules* **2001**, *34*, 7427–7434; d) T. Funami, M. Hiroe, S. Noda, I. Asai, S. Ikeda, K. Nishinari, *Food Hydrocolloids* **2007**, *21*, 617–629; e) B. T. Nguyen, T. Nicolai, L. Benyahia, C. Chassenieux, *Carbohydr. Polym.* **2014**, *112*, 10–15.

[6] C. A. Running, R. Falshaw, S. Janaswamy, *Carbohydr. Polym.* **2012**, *87*, 2735–2739.

[7] E. Wildermuth, H. Stark, G. Friedrich, F. L. Ebenhöch, B. Küborth, J. Silver, R. Rituper in *Ullmann's Encyclopedia of Industrial Chemistry*, Wiley-VCH, Weinheim, **2000**, pp. 41–62.

[8] a) *Guidelines on Food Fortification with Micronutrients* (Eds.: L. Allen, B. de Benoist, O. Dary, R. Hurrell), World Health Organization and Food and Agriculture Organization of the United Nations, Geneva, **2006**; b) F. M. Hilty, M. Arnold, M. Hilbe, A. Teleki, J. T. N. Knijnenburg, F. Ehrensperger, R. F. Hurrell, S. E. Pratsinis, W. Langhans, M. B. Zimmermann, *Nat. Nanotechnol.* **2010**, *5*, 374–380.

[9] a) Y. Fang, J. H. Hoh, *J. Am. Chem. Soc.* **1998**, *120*, 8903–8909; b) V. Andrushchenko, Z. Leonenko, D. Cramb, H. van de Sande, H. Wieser, *Biopolymers* **2002**, *61*, 243–260.

[10] a) L. L. Stookey, *Anal. Chem.* **1970**, *42*, 779–781; b) P. Carter, *Anal. Biochem.* **1971**, *40*, 450–458.

[11] J. T. Woods, M. G. Mellon, *Ind. Eng. Chem.* **1941**, *33*, 551–554.

[12] S. J. J. Debon, R. F. Tester, *Food Chem.* **2001**, *73*, 401–410.

[13] K. L. Haas, K. J. Franz, *Chem. Rev.* **2009**, *109*, 4921–4960.

[14] a) C. A. Mak, S. Ranjbar, P. Riente, C. Rodríguez-Escrich, M. A. Pericàs, *Tetrahedron* **2014**, *70*, 6169–6173; b) S. Rostamnia, B. Zeynizadeh, E. Doustkhah, A. Baghban, K. O. Aghbash, *Catal. Commun.* **2015**, *68*, 77–83.

[15] a) J. S. Sander, R. M. Erb, C. Denier, A. R. Studart, *Adv. Mater.* **2012**, *24*, 2582–2587; b) S. Fusco, M. S. Sakar, S. Kennedy, C. Peters, R. Bottani, F. Starsich, A. Mao, G. A. Sotiriou, S. Pané, S. E. Pratsinis, D. Mooney, B. J. Nelson, *Adv. Mater.* **2014**, *26*, 952–957.

[16] a) A. L. Daniel-da-Silva, S. Fateixa, A. J. Guiomar, B. F. O. Costa, N. J. O. Silva, T. Trindade, B. J. Goodfellow, A. M. Gil, *Nanotechnology* **2009**, *20*, 355602; b) K. Oya, T. Tsuru, Y. Teramoto, Y. Nishio, *Polym. J.* **2013**, *45*, 824–833.

[17] a) T. Mitsumata, A. Honda, H. Kanazawa, M. Kawai, *J. Phys. Chem. B* **2012**, *116*, 12341–12348; b) A. L. Daniel-da-Silva, J. Moreira, R. Neto, A. C. Estrada, A. M. Gil, T. Trindade, *Carbohydr. Polym.* **2012**, *87*, 328–335; c) J. J. Vallooran, R. Negrini, R. Mezzenga, *Langmuir* **2013**, *29*, 999–1004; d) S. Bolisetty, J. J. Vallooran, J. Adamcik, R. Mezzenga, *ACS Nano* **2013**, *7*, 6146–6155.

[18] I. Usov, R. Mezzenga, *Macromolecules* **2015**, *48*, 1269–1280.

[19] A. Bettini, M. R. Pozzan, E. Valdevit, C. Frontali, *Biopolymers* **1980**, *19*, 1689–1694.

[20] K. Okoshi, S.-i. Sakurai, S. Ohsawa, J. Kumaki, E. Yashima, *Angew. Chem. Int. Ed.* **2006**, *45*, 8173–8176; *Angew. Chem.* **2006**, *118*, 8353–8356.

[21] a) T. T. Perkins, D. E. Smith, R. G. Larson, S. Chu, *Science* **1995**, *268*, 83–87; b) M. D. Wang, H. Yin, R. Landick, J. Gelles, S. M. Block, *Biophys. J.* **1997**, *72*, 1335–1346; c) B. Maier, U. Seifert, J. O. Rädler, *Europhys. Lett.* **2002**, *60*, 622–628.

Received: July 25, 2015